Asymmetric intermixing in a Co–Al thin film system: An investigation using coaxial impact collision ion scattering spectroscopy

H. M. Hwang, J. Y. Park, S. K. Jung, J. Lee, and C. N. Whang[a)]
Institute of Physics and Applied Physics, Yonsei University, Seoul, 120-749, Korea

S.-P. Kim,[b)] S.-C. Lee, and K.-R. Lee[c)]
Future Technology Research Division, Korea Institute of Science and Technology, Seoul, 130-650, Korea

Y.-C. Chung
Department of Ceramic Engineering, Hanyang University, Seoul, 133-791, Korea

(Received 8 December 2006; accepted 9 March 2007; published online 14 May 2007)

Surface structure evolution during atomic deposition in a Co–Al system was investigated using coaxial impact collision ion scattering spectroscopy (CAICISS). Half monolayer of Al and Co atoms were deposited on Co(0001) and Al(001) single crystal surfaces, respectively, in an ultrahigh-vacuum environment. CAICISS analysis of the deposited surface revealed an asymmetric interfacial reaction, as predicted by previous molecular dynamics simulations. Al atoms deposited on a Co substrate are placed on the surface with no interatomic intermixing. In contrast, significant surface intermixing with the deposited Co atoms occurs on the Al(001) substrate, resulting in the formation of a CoAl intermetallic surface layer of B2 structure. These asymmetric features would be important to the understanding of the structural evolution of thin film multilayers. © *2007 American Institute of Physics*. [DOI: 10.1063/1.2730562]

I. INTRODUCTION

Thin multilayer structures are widely used in many advanced devices and sensors. Typical examples are the spintronic devices based on tunneling magneto resistance (TMR) or giant magneto resistance (GMR) phenomena.[1] These devices are composed of very thin ferromagnetic and nonmagnetic layers with thicknesses of a few nanometers. It is observed that the electromagnetic properties are largely dependent on the interfacial structure of the multilayer.[2–5] Because of the short coherence length of spin polarization, electric spin phenomena can occur only across ordered thin films of a few nanometers thickness.[6,7] It must be further noted that the interface structure limits diffusive electrical spin-injection efficiency across a heteroexpitaxial interface.[6] Control of the interface on atomic scales is thus essential for these devices and requires an in-depth understanding of the atomistic behavior during the early stages of thin film deposition.

Considerable effort using many surface analysis techniques was made to elucidate the surface structure evolution during thin film deposition.[3–5,8–13] Atomic exchange and atomic migrations on the surface are extensively reported in a variety of thin film systems. It has also been reported that the interfacial reaction in some thin film systems appear to be asymmetric. For example, Buchanan *et al.* reported an asymmetric interfacial intermixing behavior in Al−*X* multilayers, where *X* represents the transition metals from rows 4–6 of the Periodic Table.[13] They observed that the intermixing was considerably less when Al was sputtered onto the metal *X* than when *X* was deposited on Al. Asymmetric surface intermixing has also been observed in many other metal thin film systems, such as Fe–Cr,[8] Ge–Au,[12] and Co–Cu.[4]

Asymmetry in Co–Al,[14,15] Co–Cu,[16] and Au–Pt (Ref. 17) systems is predicted by empirical molecular dynamics (MD) simulations. We previously investigated the atomic scale deposition behavior in a Co–Al system, which showed asymmetric interfacial intermixing at room temperature.[14,15] When Al atoms of kinetic energy 0.1 eV were deposited on a Co substrate, they were placed on the substrate surface without surface intermixing. This behavior was observed regardless of the substrate orientation, provided the kinetic energy of the Al atoms was less than 5.0 eV. Thus, an atomically sharp interface is predicted to form between the Al thin film and the Co substrate in most evaporation or sputtering environments. In contrast, when Co atoms of kinetic energy 0.1 eV are deposited on an Al substrate, significant intermixing occurs on the Al surface. Surface intermixing was generally observed on the Al substrate regardless of the orientation. The structure of the intermixing layer was dependent on the substrate orientation. A crystalline CoAl layer of B2 structure was formed only on (001) surfaces, whereas amorphous CoAl layers evolved on (011) and (111) surfaces. The highly ordered B2 structure on the Al (001) surface may result from a small lattice mismatch ($<0.1\%$) between the CoAl B2 phase and the substrate.[14]

In the present work, we report experimental observations of the asymmetric evolution of the surface structure in a Co–Al system using coaxial impact collision ion scattering spectroscopy (CAICISS). CAICISS has been successfully used to investigate the surface structure evolution during atomic adsorption on metal substrates, as well as on crystalline Si.[18–20] Half monolayer (0.5 ML) of Al and Co atoms was deposited on Co(0001) and Al(001) single crystal sur-

[a)]Electronic mail: cnwhang@yonsei.ac.kr
[b)]Also at: Department of Ceramic Engineering, Hanyang University, Seoul, 133-791, Korea.
[c)]Electronic mail: krlee@kist.re.kr

faces, respectively, in an ultrahigh-vacuum environment. The CAICISS analysis revealed that asymmetric intermixing occurs in Co–Al systems, as was predicted by empirical MD simulations.[14,15]

II. EXPERIMENTAL

The deposition and CAICISS experiments were performed at room temperature in an ultrahigh-vacuum chamber with a base pressure of around 10^{-10} Torr. Mirror-polished Co(0001) and Al(001) single crystals of diameter 10 mm were used as the substrate. Before the deposition, the surface residues were removed by sputtering with 2.0 keV Ar^+ ion beam. The specimens were then annealed at 650 K for 1 to 2 h to relax the surface structure. These processes were repeated several times until a clean substrate surface appeared as judged by the presence of bright low energy electron diffraction (LEED) patterns. A half monolayer of the adatoms (3.4×10^{14} atoms/cm^{-2}) was deposited by thermal evaporation. Co atoms were supplied using a heated pure Co wire and Al atoms were evaporated using a heated W filament. From the melting temperature of Co and Al, the kinetic energy of the adatoms is expected to be around 0.1 eV, which is similar to that in the MD simulations.[14,15]

For the CAICISS measurement, 3 keV He^+ ions of beam current 10 pA were irradiated on the surface at a specific angle. The ion flux with this beam current is estimated to be 1.79×10^{12} cm^2 h. Thus, there would be negligible damage to the sample because of the irradiation. A time-of-flight (TOF) mode analyzer was used to measure the energy of the backscattered He particles. Yields of He particles scattered by the substrate atoms were measured under polar- and azimuthal-scan conditions. Details of the CAICISS measurement were reported in previous publications.[21,22] We used a two-dimensional trajectory count method using the Ziegler-Biersack-Littmark (ZBL) potential to simulate the scattering spectrum.[23,24]

III. RESULTS AND DISCUSSION

A. Al atoms on a Co (0001) surface

Figure 1(a) shows the azimuthal-scan curves for clean Co (0001) at an incidence angle of 13°. We took the $[1\bar{1}00]$ direction as the origin of the azimuthal scan. A simulated scattering curve is also included for comparison in Fig. 1(a). The shape of the measured spectrum agrees well with the characteristics of the simulated one, even though the peaks in the experimental observation are smeared because of thermal vibrations or surface defects. The experimental curve shown in Fig. 1(b) is the azimuthal-scan curve after depositing a 0.5 ML Al on a Co (0001) surface. The scattering yield at around 0° and 60° increased, and the other characteristics of the curve such as troughs near −30° and 30° remained unchanged. Figure 1(c) schematically shows a top view of the atomic configuration of the Co (0001) surface. Large gray circles represent the topmost atoms of the Co (0001) surface and small closed circles correspond to the atoms on the second layer. On the Co (0001) surface, there are four typical adsorption sites [marked with crosses in Fig. 1(c)]: On the top, bridge, hcp, and fcc hollow. The increased peaks at 0° and 60° result from the focusing effect of the Al adatoms adsorbed on either fcc or hcp hollow sites, because these hollow sites are aligned along the $[1\bar{1}00]$ and $[0\bar{1}10]$ directions. If Al adatoms were adsorbed on the bridge site that is aligned along the [1000] or $[0\bar{1}00]$ direction, the scattering yield at around −30° and 30° would increase. If Al adatoms were adsorbed on the on-top site, the scattering yield at all angles around −30°, 0°, 30°, and 60° would vary with the Al deposition. It is thus evident from the azimuthal scan that the Al adatoms are preferentially placed on the hollow sites if the Al atoms were placed on the top of the Co surface without intermixing.

First-principle calculations of the adsorption energy of Al atoms on a Co (0001) surface support the experimental observations. The Vienna *ab initio* calculation package (VASP) was used for the present calculations.[25,26] A fully relaxed structure of five atomic layers (45 atoms) of Co with one Al atom on the top was characterized by the spin-polarized calculation. We used a projector-augmented wave (PAW) with generalized gradient approximation (GGA) for the exchange correlation potential.[27,28] The calculated adsorption energies for the possible adsorption sites are summarized in Table I. The adsorption energy for the hollow sites is around 3.55 eV, which is quite larger than that for the other sites (3.09 eV for the on-top site and 3.40 eV for the bridge site). The energy difference between the two hollow sites is only 8.55×10^{-3} eV, which means that the Al atoms will occupy both the fcc and hcp sites at room temperature with approximately the same probability. The equilibrium height of the Al adatom from the surface Co layer was calculated to be 1.87 Å.

The solid curve in Fig. 1(b) is the simulated scattering curve for a Co (0001) surface with a 0.5 ML of Al atoms on the hollow sites. In this simulation, we assumed that half of the Al atoms are located on fcc sites and the other half on hcp sites without intermixing. The simulated curve reveals that the Al addition on the hollow sites significantly increases the scattering peaks at 0° and 60°, which agrees well with the experimental observation. The only fitting parameter in the scattering simulation was the height of the Al atoms from the surface Co layer. The simulated scattering curve in Fig. 1(b) is for a height of 1.8 Å, which also agrees with the first-principle calculation results.

Figure 2(a) shows the incidence-angle region of the polar-scan curves along the $[1\bar{1}00]$ direction for a clean Co(0001) surface and a 0.5 ML Al deposited Co(0001) surface. Because of scattering from the specimen holder at low incident angles, scattering curves are only presented for polar angles larger than 10°. The most noteworthy difference between the clean and Al adsorbed Co surface is the enhanced scattering peak near 37°. There is also a slight increase in the scattering yield near 20° and 34°. Features of the polar-scan curve are consistent with those of the simulated curve [solid curve in Fig. 2(a)], with the enhanced scattering peaks near 37° and 20° being clearly present in the simulated curve. The simulated curve was obtained under the assumption that the adsorbed Al atoms are placed on both hcp and fcc hollow sites with the same probability and the height of the adsorbed Al atom is 1.80 Å.

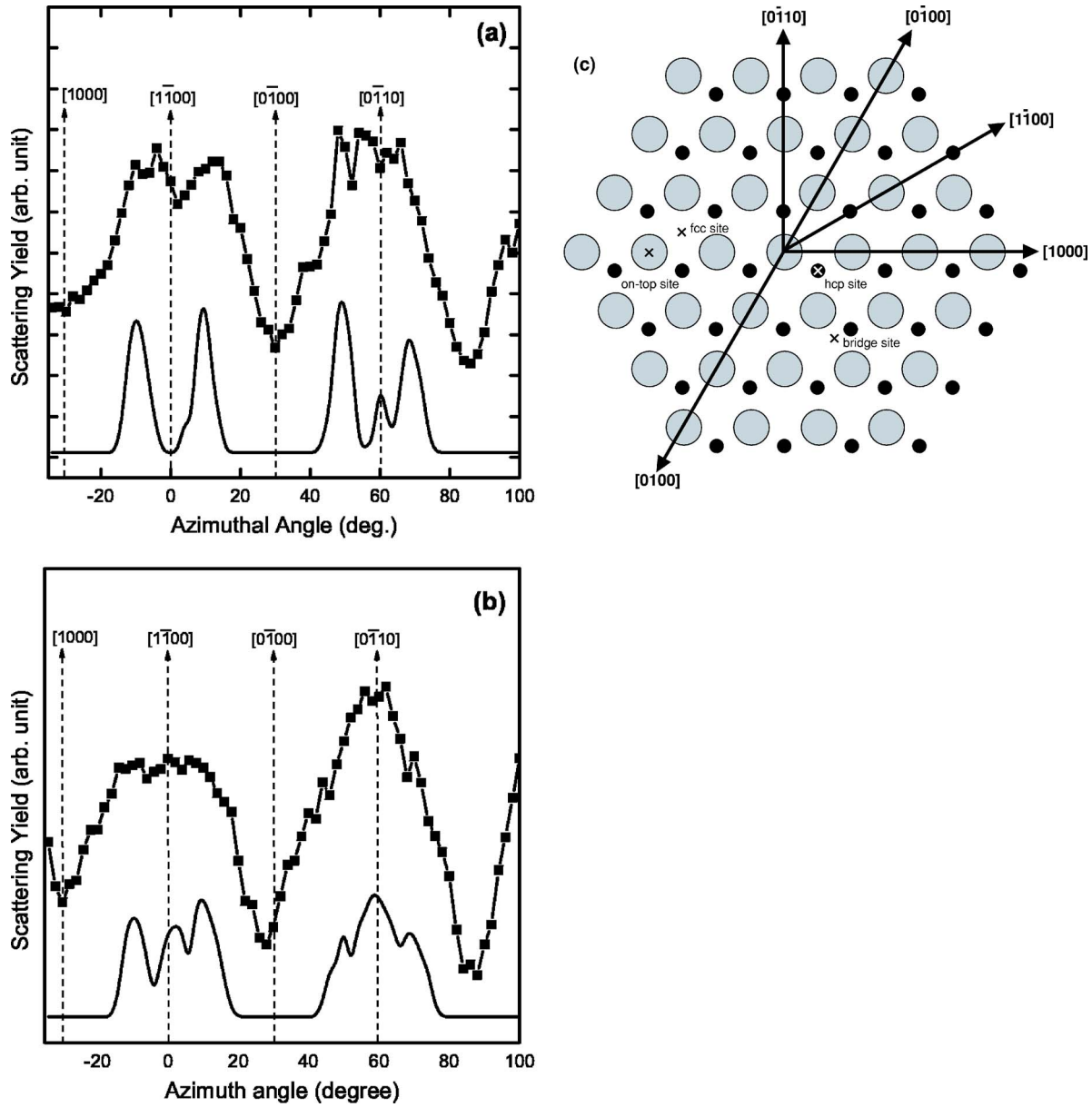

FIG. 1. (Color online) (a) Azimuthal-scan curves of the He yield backscattered by Co atoms at an incidence angle of 13° for a clean Co (0001) surface (solid square data) and the simulated scattering curve (solid line curve). (b) Azimuthal-scan curves of the He yield scattered by Co atoms at an incidence angle of 13° for a 0.5 ML Al deposited Co (0001) surface (solid square data) and the simulated scattering curve when the deposited Al atoms are placed on the hollow sites at a height of 1.8 Å from the first layer of Co (solid line curve). (c) Top view of the atomic configuration of a Co (0001) surface. Large gray circles are the atoms in the first layer and small solid circles are the atoms in the second layer. Crosses indicate the surface sites: On-top site, bridge site, and two hollow (fcc and hcp) sites.

TABLE I. Adsorption energies and characteristic geometry of the Al/Co (0001) system.

Position of adatom	E_{ad} [a] (eV)	ΔE_{hcp} [b] (meV)	d_{as} [c] (Å)
hcp hollow site	3.55698	0.0	1.87±0.01
fcc hollow site	3.54834	8.55	1.87±0.02
On-top site	3.09436	462.53	2.22±0.01
Bridge site	3.39614	160.75	1.84±0.02

[a] E_{ad} is the adsorption energy $[E_{ad}=E_{total}(\text{Co\_surface})+E_{total}(\text{Al\_atom})-E_{total}^{ad\_site}(\text{Al/Co})]$.
[b] ΔE_{hcp} is the difference in the adsorption energy with respect to the hcp hollow site.
[c] d_{as} is the height of the Al adatom from the surface Co layer.

Figure 2(b) shows the in-depth schematic atomic configuration along the [1$\bar{1}$00] direction with adsorbed Al atoms on both hcp and fcc hollow sites. Details of the polar-scan curve can be characterized in terms of the focusing effect of the adsorbed Al atoms. The increased scattering yield at around 20° can be explained by the focusing effect between Al atoms on the hcp site and Co atoms of the first layer of the substrate [denoted by $A_{1'}$, in Fig. 2(b)]. Scattering yields at around 18° and 33° arise from the focusing effect between Al atoms on the hcp site and the Co atoms of the first and/or the second layer [denoted by A_1, $A_{2'}$, and A_2 in Fig. 2(b)]. Al atoms on the fcc sites induce a focusing effect on the Co atoms of the second layer [denoted by $A_{2'}$ in Fig. 2(b)], which enhances the scattering yield at around 22° and 37°. In

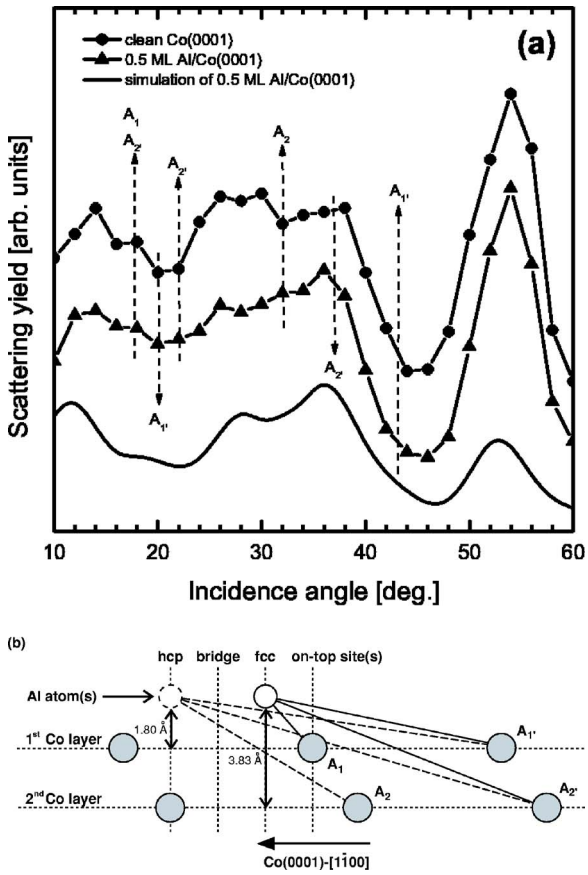

FIG. 2. (Color online) (a) Polar scan curves of the He yield backscattered by Co atoms along the [1$\bar{1}$00] direction for a clean Co (0001) surface (solid circle data), a 0.5 ML Al deposited Co (0001) surface (solid triangle data) and the simulated scattering curve when the deposited Al atoms are placed on the hollow sites at a height of 1.8 Å from the first layer of Co (solid line curve). (b) Side view along the[1$\bar{1}$00] direction of the model structure when the deposited Al atoms are placed on both the fcc and hcp hollow sites of the Co (0001) surface.

addition, the focusing effect between Al atoms on the fcc site and the Co atoms of the first layer can increase the yield at around 44° [denoted by $A_{1'}$ in Fig. 2(b)]; however, this increase is not evident in the experimental spectrum. The reason for this discrepancy is not clear but is presumably due to surface defects.

B. Co atoms on an Al (001) surface

In contrast to the Al deposited Co surface where adatoms are deposited on the substrate surface without surface intermixing, Co deposition on an Al surface shows a surface alloy structure resulting from surface intermixing. Figures 3(a) and 3(b) show the azimuthal-scan curves for a clean Al (001) surface and a 0.5 ML Co deposited Al (001) surface at an incidence angle of 13°. We used the [110] direction as the origin of the azimuthal scan. The scattering curve for a clean Al (001) surface appears symmetric with respect to the azimuthal angle of 45° because of the mirror symmetry in atomic configuration with respect to the [010] direction. Major peaks of the clean surface near 20° and 40° coincide closely with those of the simulated scattering curve [solid line curve in Fig. 3(a)], despite the experimentally observed scattering peaks being quite smeared. 0.5 ML Co deposited

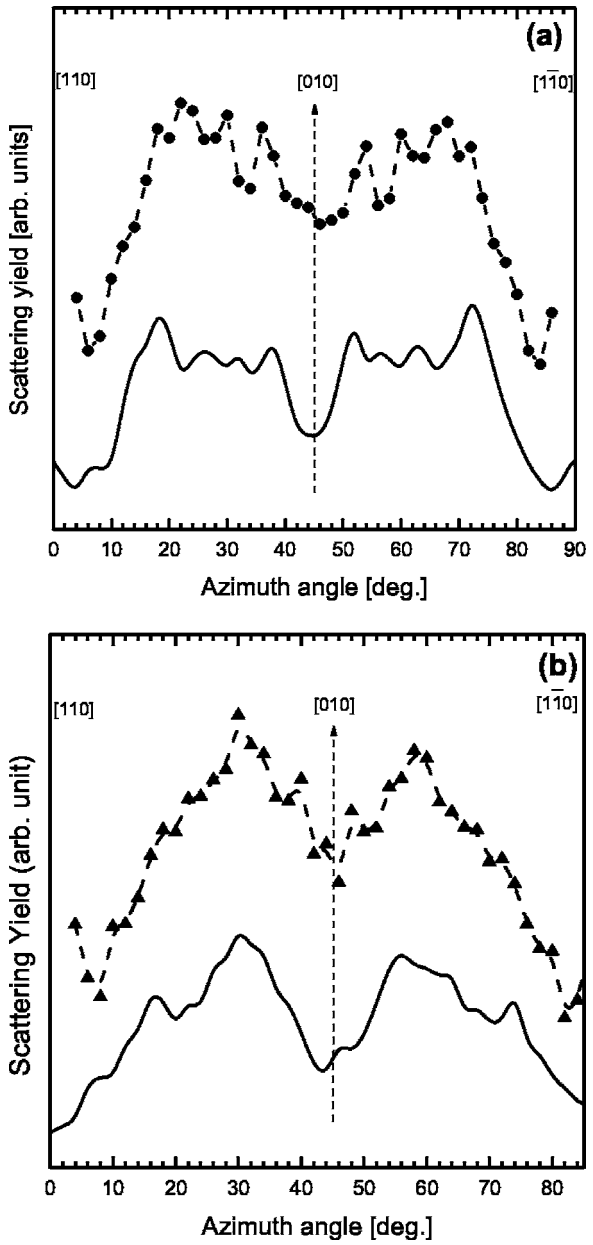

FIG. 3. (a) Azimuthal-scan curves of the He yield backscattered by Al atoms at an incidence angle of 13° for a clean Al (001) surface (solid square data) and the simulated scattering curve (solid line curve). (b) Azimuthal-scan curves of the He yield scattered by Al atoms at an incidence angle of 13° for a 0.5 ML Co deposited Al (001) surface (solid square data) and the simulated scattering curve of CoAl B2 structure with an Al top layer (solid line curve).

Al surface produced the scattering curve shown in Fig. 3(b). Two broad peaks appear near 30° and 56°, and most of the peaks of the clean Al surface disappear. However, the scattering curve is similar to the simulated scattering curve of a CoAl B2 (001) surface with an Al top layer [(solid line curve in Fig. 3(b)]. The agreement between the simulated and experimentally observed curves shows that a CoAl intermetallic phase formed on the surface. The intermetallic phase is formed only through severe atomistic intermixing on the Al substrate surface during Co deposition.

Formation of a CoAl intermetallic surface layer is more evident in the polar-scan curve. Figure 4(a) shows the

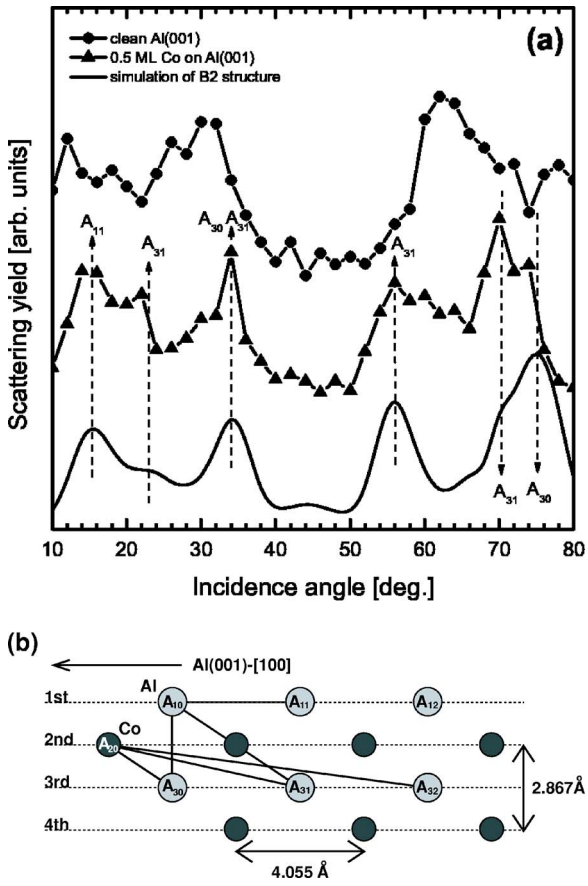

FIG. 4. (Color online) (a) Polar-scan curves of the He yield backscattered by Al atoms along the [100] direction for a clean Al (001) surface (solid circle data), a 0.5 ML Co deposited Al (001) surface (solid triangle data) and the simulated scattering curve of CoAl B2 structure with an Al top layer (solid line curve). (b) Side view along the [100] direction of a CoAl B2 structure with an Al top layer.

incidence-angle region of the polar-scan curves along the [100] direction of an Al substrate. A clean Al (001) surface without Co atoms on the surface exhibits major scattering peaks near 12°, 30°, and 62°. Beyond 62°, the scattering yield gradually decreases except for a small peak near 78°. However, Co deposition on the Al surface entirely changed the shape of the scattering curve. The peaks at 12° and 30° disappeared, whereas new peaks near 16°, 22°, and 36° appeared. Furthermore, new peaks near 56° and 71° appeared with a trough near 65° where the clean Al (001) surface has a scattering peak near 62°. These new peaks coincide closely with the simulated scattering peaks of a (001) surface of CoAl B2 phase with an Al top layer [solid line curve in Fig. 4(a)]. The in-depth schematic atom configuration along [100] direction of the B2 phase used in the simulation is shown in Fig. 4(b). However, the scattering behavior at higher polar angles ranging from 70° to 80° exhibits a large discrepancy from the simulated behavior, and this is discussed below.

Details of the polar-scan curve can be explained in terms of the focusing effect of the surface atoms. The scattering peak near 16° originates from the focusing effect between the surface Al atoms [the atoms denoted by A_{10}, A_{11}, and A_{12} in Fig. 4(b)]. The surface Al atoms can also have another focusing effect on the Al atoms in the third layer, which results in an increased scattering yield at higher polar angles such as at 71° because of the focusing effect between the A_{10} and A_{31} atoms, or at 75° because of the effect between the A_{10} and A_{30} atoms. Although the scattering yield at 71° is expected to be weak for a perfect B2 phase because of the screening effect of the Co atoms in the second layer, the experimental scattering yield near 71° was significantly higher. This difference shows that the amount of B2 structure formed by deposition of a 0.5 ML of Co is not sufficient to change the entire surface to a CoAl intermetallic phase. In addition, the B2 surface layer has a high degree of defects as appeared in the MD simulations.[14,15] The Co atoms in the second layer also induce a focusing effect with Al atoms in the third layer. For example, a focusing effect between A_{20} and A_{30} or A_{31} induces the scattering peak near 34°, and the focusing effect between A_{20} and A_{31} or A_{32} results in scattering peaks near 56° and 19°.

It is worth comparing the behavior when Co is deposited on an Al (001) surface with that observed when Al is deposited on a Co (0001) surface. In the latter case, both the polar- and azimuthal-scan curves show slight changes in the scattering peaks with an almost identical shape on larger scales (see Figs. 1 and 2). The slight change originates from the fact that the adsorbed Al atoms are located on the fcc or hcp hollow sites of the Co (0001) surface without surface intermixing. On the other hand, Co deposition on an Al (001) substrate induced substantial changes in the scattering curve of both azimuthal and polar scans. The observed scattering curves are consistent with the simulated scattering curves of a CoAl B2 structure with an Al top layer. This surface layer results from the atomic scale intermixing on the Al substrate during deposition of Co. The observed behavior of asymmetric surface intermixing strongly supports the predictions of the MD simulations.[14,15]

IV. CONCLUSIONS

Asymmetry of the surface intermixing in a Co–Al system was experimentally observed using the CAICISS method with single crystal substrates. The present work is consistent with previous results from empirical MD simulations. Al atoms deposited on a Co substrate are placed on the surface hollow sites without interatomic intermixing. On the other hand, significant atomic intermixing occurs on the Al surface between the deposited Co atoms and the Al substrate, resulting in the formation of a CoAl intermetallic surface layer of B2 structure on an Al (001) surface.

ACKNOWLEDGMENTS

The authors gratefully acknowledge the support and critical advice of Dr. J.-H. Song and Dr. K. H. Chae at the Korea Institute of Science and Technology. Work undertaken at Yonsei University was financially supported in part by the Brain Korea 21 project of Korea Research Foundation, and the Korea Science and Engineering Foundation through the National Core Research Center for Nanomedical Technology at Yonsei University. H.M.H. and J.L. were supported by a Korea Research Foundation Grant No. KRF-2004–015-C00170, and by Grant No. R01–2004–000–10715–0 from the Basic Research Program of the Korea Science and Engi-

neering Foundation. Work undertaken at KIST was financially supported by the KIST core capability enhancement program, Contract Nos. 2V00910 and 2E19190.

[1]K. Inomata and Y. Saito, J. Appl. Phys. **81**, 5344 (1997).
[2]H. Wieldraaijer, P. LeClair, J. T. Kohlhepp, H. J. M. Swagten, and W. J. M. de Jonge, IEEE Trans. Magn. **38**, 2727 (2002).
[3]N. R. Shivaparan, M. A. Teter, and R. J. Smith, Surf. Sci. **476**, 152 (2001).
[4]D. J. Larson, A. K. Petford-Long, Y. Q. Ma, and A. Cerezo, Acta Mater. **52**, 2847 (2004).
[5]T. Mitsuzuka, A. Kamijo, and H. Igarashi, J. Appl. Phys. **68**, 1787 (1990).
[6]R. M. Stroud, A. T. Hanbicki, Y. D. Park, G. Kioseoglou, A. G. Petukhov, B. T. Jonker, G. Itskos, and A. Petrou, Phys. Rev. Lett. **89**, 166602 (2002).
[7]J. M. De Teresa, A. Barthélémy, A. Fert, J. P. Contour, F. Montaigne, and P. Seneor, Science **286**, 507 (1999).
[8]U. Mick, V. Uzdin, and E. Kisker, J. Magn. Magn. Mater. **240**, 398 (2002).
[9]S. H. Kim, Y. Jikeun, S. Shin, W. Kim, C. Y. Park, S.-J. Oh, J. M. Seo, H. G. Min, and J.-S. Kim, Phys. Rev. B **63**, 085414 (2001).
[10]J. Kim, J.-W. Lee, J.-R. Jeong, S.-C. Shin, Y. H. Ha, Y. Park, and D. W. Moon, Phys. Rev. B **65**, 104428 (2002).
[11]S. Rousset, S. Chiang, D. E. Fowler, and D. D. Chambliss, Phys. Rev. Lett. **69**, 3200 (1992).
[12]M. W. Ruckman, J. J. Joyce, F. Boscherini, and J. H. Weaver, Phys. Rev. B **34**, 5118 (1986).
[13]J. D. R. Buchanan, T. P. A. Hase, B. K. Tanner, P. J. Chen, L. Gan, C. J. Powell, and W. F. Egelhoff, Jr., Phys. Rev. B **66**, 104427 (2002).
[14]S.-P. Kim, Y.-C. Chung, S.-C. Lee, K.-R. Lee, and K.-H. Lee, J. Appl. Phys. **93**, 8564 (2003).
[15]S.-P. Kim, S.-C. Lee, K.-R. Lee, and Y.-C. Chung, J. Electroceram. **13**, 315 (2004).
[16]X. W. Zhou, H. N. G. Wadley, R. A. Johnson, D. J. Larson, N. Tabat, A. Cerezo, A. K. Petford-long, G. D. W. Smith, P. H. Clifton, R. L. Martens, and T. F. Kelly, Acta Mater. **49**, 4005 (2001).
[17]M. I. Haftel, M. Rosen, T. Franklin, and M. Hettermann, Phys. Rev. B **53**, 8007 (1996).
[18]M. Aono, M. Katayama, T. Chesse, D. S. Choi, and M. Kato, Nucl. Instrum. Methods Phys. Res. B **37-38**, 264 (1989).
[19]J. H. Seo, J. Y. Park, S. K. Jung, K.-H. Yoo, C. N. Whang, S. S. Kim, D. S. Choi, and K. H. Chae, Chem. Phys. Lett. **417**, 72 (2006).
[20]M. Walker, C. R. Parkinson, M. Draxler, and C. F. McConville, Surf. Sci. **584**, 153 (2005).
[21]W. S. Cho, J. Y. Kim, S. S. Kim, D. S. Choi, K. Jeong, I. W. Lyo, C. N. Whang, and K. H. Chae, Surf. Sci. Lett. **476**, L259 (2001).
[22]W. S. Cho, J. Y. Kim, N. G. Park, I. W. Lyo, K. Jeong, S. S. Kim, D. S. Choi, C. N. Whang, and K. H. Chae, Surf. Sci. Lett. **453**, L309 (2000).
[23]J. F. Ziegler, J. P. Biersack, and U. Littmark, *Stopping Powers and Ranges of Ions in Matter* (Pergamon, New York, 1985).
[24]J. P. Biersack, Nucl. Instrum. Methods Phys. Res. B **27**, 21 (1987).
[25]G. Kresse and J. Furthmuller, *Vienna ab initio Simulation Package* (University of Vienna, Vienna, 2001).
[26]G. Kresse and J. Hafner, Phys. Rev. B **47**, 558 (1993).
[27]G. Kresse and J. Joubert, Phys. Rev. B **59**, 1758 (1999).
[28]J. P. Perdew, K. Burke, and M. Ernzerhof, Phys. Rev. Lett. **77**, 3865 (1996).